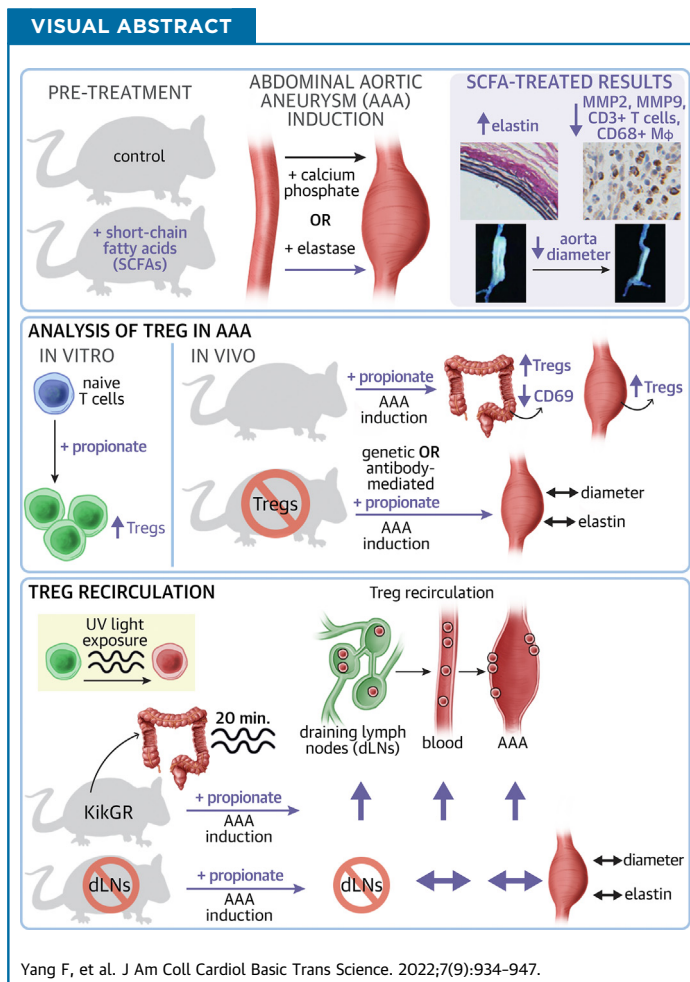


ORIGINAL RESEARCH - PRECLINICAL

Propionate Alleviates Abdominal Aortic Aneurysm by Modulating Colonic Regulatory T-Cell Expansion and Recirculation



Fen Yang, MD,^{a,*} Ni Xia, MD, PhD,^{a,*} Shuang Guo, MD,^{a,*} Jiyu Zhang, MS,^a Yuhan Liao, MS,^a Tingting Tang, MD, PhD,^a Shaofang Nie, MD, PhD,^a Min Zhang, MD, PhD,^a Bingjie Lv, MD,^a Yuzhi Lu, MD, PhD,^a Jiao Jiao, MD, PhD,^a Jingyong Li, MD, PhD,^a Weimin Wang, PhD,^b Desheng Hu, MD, PhD,^c Xiang Cheng, MD, PhD^a



HIGHLIGHTS

- SCFAs alleviate the progression of AAA in both $\text{Ca}_3(\text{PO}_4)_2$ - and elastase-induced mouse AAA models.
- Propionate expands the pool of Tregs in the cLP and enhances the cell-intrinsic ability of cLP-Tregs to recirculate by downregulating CD69 expression on the surface of cLP-Tregs.
- Propionate facilitates the recirculation of cLP-Tregs from the cLP through colonic dLNs and circulating blood to the inflamed aneurysm to mitigate AAA.

SUMMARY

Emerging evidence supports that intestinal microbial metabolite short-chain fatty acids (SCFAs) increase the pool of regulatory T cells (Tregs) in the colonic lamina propria (cLP) and protect against nonintestinal-inflammatory diseases, such as atherosclerosis and post-infarction myocardial inflammation. However, whether and how SCFAs protect the inflamed aortas of subjects with abdominal aortic aneurysm (AAA) remains unclear. Here, the authors revealed the protective effect of SCFAs on AAA in mice and the expansion of Tregs in the cLP, and propionate exerted Treg-dependent protection against AAA by promoting the recirculation of cLP-Tregs through colonic draining lymph nodes (dLNs) to the inflamed aorta. (J Am Coll Cardiol Basic Trans Science 2022;7:934-947) © 2022 The Authors. Published by Elsevier on behalf of the American College of Cardiology Foundation. This is an open access article under the CC BY-NC-ND license (<http://creativecommons.org/licenses/by-nc-nd/4.0/>).

Abdominal aortic aneurysm (AAA) refers to the deterioration and dilatation of the abdominal aorta and manifests as a diameter increase of more than 50%. Clinically, aortic deterioration and expansion progress asymptotically until lethal rupture, which results in a mortality rate of 85% to 90%.¹ The pathology of AAA involves chronic inflammation, apoptosis of vascular smooth muscle cells, and degradation of the extracellular matrix. Inflammation triggers deterioration of the aorta, whereas fragments of the degraded aortic wall in turn recruit proinflammatory monocytes/macrophages and T cells, which produce proteases, especially matrix metalloproteinase (MMP)-2 and -9, causing further damage to the aortic wall.^{2,3} Among infiltrating immune cells, regulatory T cells (Tregs) modulate inflammation by secreting anti-inflammatory cytokines and inhibiting proinflammatory macrophages.^{4,5} Despite recent advances in pathophysiology, AAA remains a threat in the elderly population. However, no medication can be prescribed to prevent the progression of AAA.⁶ Inhibiting chronic and excessive inflammation in subjects with AAA may be a strategy for restricting aortic expansion.

Increasing evidence suggests that the intestinal microbiota plays a role in inflammatory cardiovascular diseases.⁷ The microbiota regulates the host immune system by producing active metabolites in the intestine, among which short-chain fatty acids (SCFAs) are

attracting interest.⁸ SCFAs, mainly acetate, propionate, and butyrate, which are products of bacterial fermentation of dietary fiber in the colon, have been reported to alleviate inflammatory bowel diseases by expanding Tregs.⁹⁻¹¹ Beyond the actions reported in intestinal immune homeostasis, SCFAs have been found to play critical roles in nonintestinal inflammatory disorders, such as hypertension,^{12,13} atherosclerosis,^{14,15} and myocardial infarction.¹⁶ However, whether and how SCFAs modulate AAA remains unclear.

In the present study, we aimed to identify whether and how SCFAs influence AAA. We confirmed the protective effect of SCFAs in both Ca₃(PO₄)₂-induced and elastase-induced mouse models of AAA and subsequently elucidated the underlying mechanisms by focusing on how a representative and potent SCFA, propionate, mitigated AAA. Our results highlight the prominent role of SCFAs in aortic inflammation and provide a basis for the development and translation of prebiotic-based therapeutics for human AAA.

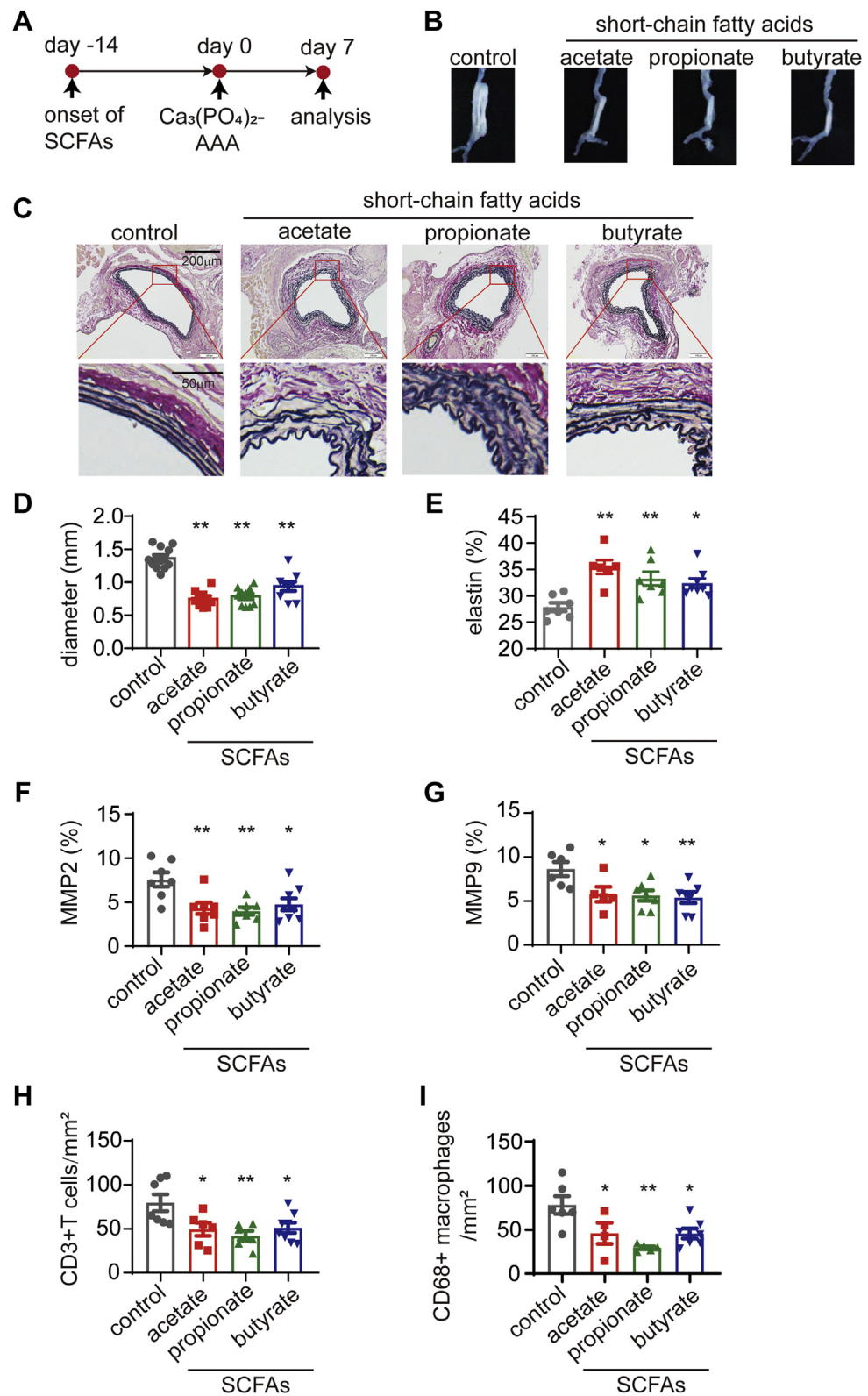
METHODS

ETHICS. All mice studies were approved by the Animal Care and Utilization Committee of Huazhong University of Science and Technology (number [2017]-

ABBREVIATIONS AND ACRONYMS

- AAA** = abdominal aortic aneurysm
- ANOVA** = analysis of variance
- CCR** = C-C chemokine receptor
- cLP** = colonic lamina propria
- DEREG** = depletion of regulatory T cell
- dLN** = draining lymph node
- DT** = diphtheria toxin
- EVG** = Elastica van Gieson
- IgG** = immunoglobulin G
- MMP** = matrix metalloproteinase
- PBS** = phosphate-buffered saline
- pHC** = photoconversion
- SCFA** = short-chain fatty acid
- SI-LP** = small intestinal lamina propria
- SPF** = specific pathogen-free
- Treg** = regulatory T cell

From the ^aDepartment of Cardiology, Union Hospital, Tongji Medical College, Huazhong University of Science and Technology, and Key Laboratory of Biological Targeted Therapy of the Ministry of Education, Wuhan, China; ^bDepartment of Immunology, School of Basic Medicine, Tongji Medical College, Huazhong University of Science and Technology, Wuhan, China; and the ^cDepartment of Integrated Traditional Chinese and Western Medicine, Union Hospital, Tongji Medical College, Huazhong University of Science and Technology, Wuhan, China. *Drs Yang, Xia, and Guo contributed equally to this work. The authors attest they are in compliance with human studies committees and animal welfare regulations of the authors' institutions and Food and Drug Administration guidelines, including patient consent where appropriate. For more information, visit the [Author Center](#).

FIGURE 1 SCFAs Alleviate the Progression of $\text{Ca}_3(\text{PO}_4)_2$ -Induced AAA

S100). All procedures were conducted in accordance with the National Institutes of Health guidelines.

AAA MODELS. Male mice were used. Mice were anesthetized with isoflurane. Elastase-induced AAA was performed as previously described.¹⁷ Briefly, the infrarenal region of abdominal aorta was exposed under stereomicroscope, and a small piece of gauze soaked with 10 μ L of porcine pancreatic elastase (E1250, Sigma-Aldrich) was applied around the aorta for 10 minutes. $\text{Ca}_3(\text{PO}_4)_2$ -induced AAA was also established as previously described.¹⁸ Similarly, a piece of gauze soaked with 0.5 mol/L calcium chloride solution was applied around the aorta for 10 minutes and replaced by a piece of phosphate-buffered saline (PBS)-soaked gauze for 5 minutes. After rinsing the peritoneal cavity twice, the incision was closed with interrupted sutures. Additional details are provided in the [Supplemental Appendix](#).

STATISTICAL ANALYSIS. Statistical analyses were performed using GraphPad Prism software version 8.0 (GraphPad Software). The Kolmogorov-Smirnov test was used to assess normality, and if the data met a normal distribution, a 2-tailed unpaired Student's *t*-test was used for comparisons between 2 groups. One-way analysis of variance (ANOVA) followed by Dunnett's multiple comparisons test or 2-way ANOVA followed by Bonferroni's multiple comparisons test was used for experiments with more than 2 groups. For data that were not normally distributed, a nonparametric Mann-Whitney *U* test was used. For continuous variables that were normally distributed, results are presented as mean \pm SEM. For continuous variables that were not normally distributed, results are presented as box-whisker plots, where the boxes indicate the median values and the interquartile ranges (25th to 75th percentiles), and the whiskers represent the minimum and maximum values. A value of *P* < 0.05 was considered statistically significant.

Details regarding the extended methods are provided in the [Supplemental Materials](#).

RESULTS

SUPPLEMENTATION WITH ACETATE, PROPIONATE, OR BUTYRATE ATTENUATES $\text{Ca}_3(\text{PO}_4)_2$ -INDUCED AAA.

To demonstrate that SCFAs prevent the development of AAA, we administered sodium acetate, propionate, butyrate, or chloride (as a control) (each at 200 mmol/L) to specific pathogen-free (SPF) mice via the oral route throughout the experiment. Fourteen days after SCFA administration, AAA was induced with $\text{Ca}_3(\text{PO}_4)_2$, and the mice were sacrificed 7 days later to evaluate AAA severity ([Figure 1A](#)). No significant differences in body weights were found among the groups after SCFA treatment for 3 weeks, indicating that the mice had good SCFA tolerance ([Supplemental Figure 1A](#)). Serum triglyceride, total cholesterol, and lipoprotein levels were not altered by SCFAs ([Supplemental Figures 1B to 1E](#)).

In comparison with sodium chloride treatment, treatment with SCFAs significantly decreased the maximum outer diameter of the aneurysm ([Figures 1B and 1D](#)). Elastica van Gieson (EVG) staining showed significantly less degradation of medial elastin in the aortic wall in the SCFA groups than in the control group ([Figures 1C and 1E](#)). The expression of MMP2 and MMP9 was down-regulated by SCFAs, as measured by immunohistochemistry staining, and fewer CD3⁺ T cells and CD68⁺ macrophages were detected in SCFA-treated mice than in control mice ([Figures 1F to 1I, Supplemental Figures 2 and 3](#)).

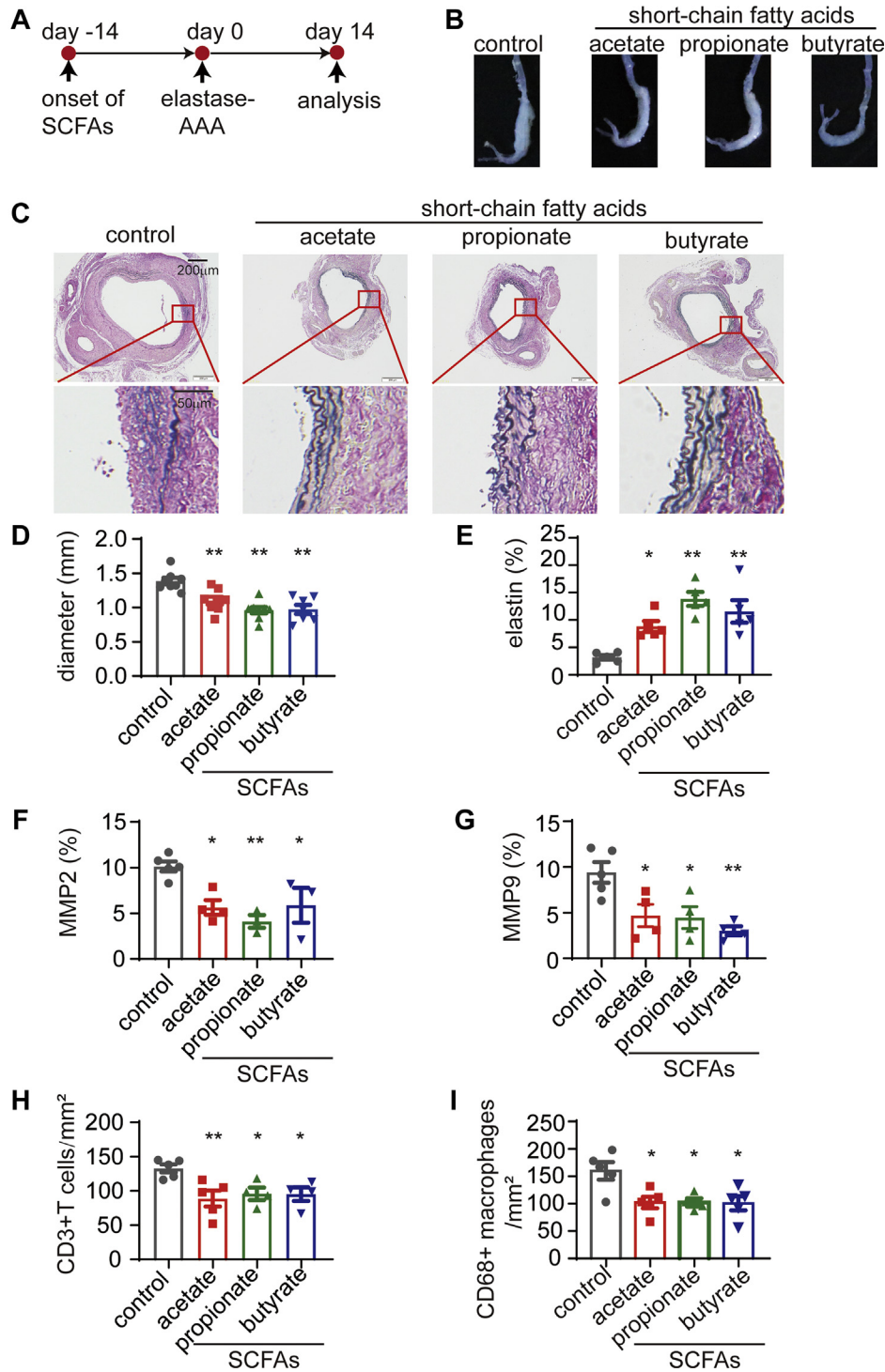
SUPPLEMENTATION WITH ACETATE, PROPIONATE, OR BUTYRATE ALSO ATTENUATES ELASTASE-INDUCED AAA.

To corroborate the protective effect of SCFAs against AAA, SCFAs were administered orally 14 days before the induction of AAA with elastase. Fourteen days after AAA induction, the mice were sacrificed to evaluate AAA severity ([Figure 2A](#)). The maximum

FIGURE 1 Continued

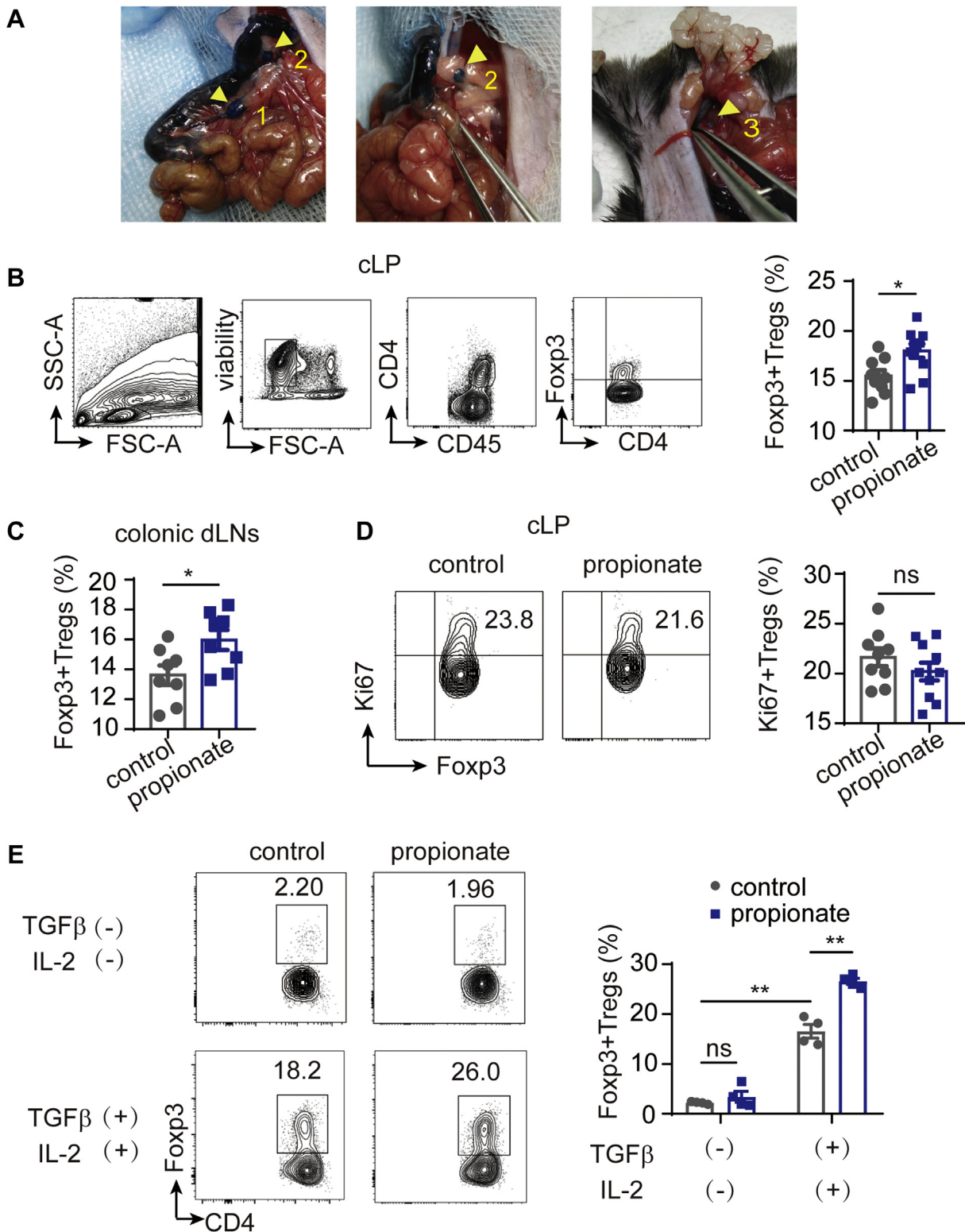
(A) Study overview: C57BL/6J mice of SPF grade were administered sodium chloride (control), acetate, propionate or butyrate via their drinking water for 14 days before the induction of AAA by $\text{Ca}_3(\text{PO}_4)_2$. The mice were sacrificed for the evaluation of severity 7 days after AAA induction. (B) Representative images of the aneurysms of mice in A. (C) Representative EVG staining of the aneurysm sections. (D) The maximum external diameters were measured ex vivo (n = 8-11). (E) The percentage of the elastin area (of the total aortic area) calculated from the EVG staining sections (n = 6-8). The percentage of the (F) MMP2-positive (n = 7-8) and (G) MMP9-positive (n = 5-7) areas (of the total aortic area) calculated from the immunohistochemistry staining sections. The mean number of (H) CD3⁺ T cells (n = 6-8) and (I) CD68⁺ macrophages (n = 4-7) per mm² of the aortic area calculated from the immunohistochemistry staining sections. Each symbol represents a value from an individual mouse. For E to I, each symbol represents the mean value of 4 to 8 consecutive sections acquired from an individual mouse. Scale bars are depicted in the images. **P* < 0.05, ***P* < 0.01. Error bars represent the mean \pm SEM. One-way ANOVA followed by Dunnett's multiple comparisons test. Data shown are representative of 2 to 3 independent experiments. AAA = abdominal aortic aneurysm; ANOVA = analysis of variance; EVG = Elastica van Gieson; SCFAs = short-chain fatty acids; SPF = specific pathogen-free.

FIGURE 2 SCFAs Alleviate the Progression of Elastase-Induced AAA



(A) Study overview: C57BL/6J mice of SPF grade were administered sodium chloride (control), acetate, propionate, or butyrate via their drinking water for 14 days before the induction of AAA by elastase. The mice were sacrificed for the evaluation of severity 14 days after AAA induction. **(B)** Representative images of the aneurysms of mice in **A**. **(C)** Representative EVG staining of the aneurysm sections. **(D)** The maximum external diameters were measured ex vivo ($n = 7-8$). **(E)** The percentage of the elastin area (of the total aortic area) calculated from the EVG staining sections ($n = 5$). The percentage of **(F)** MMP2-positive ($n = 3-5$) and **(G)** MMP9-positive ($n = 4-5$) areas (of the total aortic area) calculated from the immunohistochemistry staining sections. The mean number of **(H)** CD3⁺T cells ($n = 4-5$) and **(I)** CD68⁺ macrophages ($n = 4-5$) per mm² of the aortic area calculated from the immunohistochemistry staining sections. Each symbol represents a value from an individual mouse. For **E to I**, each symbol represents the mean value of 4 to 8 consecutive sections acquired from an individual mouse. Scale bars are depicted in the images. * $P < 0.05$, ** $P < 0.01$. Error bars represent the mean \pm SEM. One-way ANOVA followed by Dunnett's multiple comparisons test. Data shown are representative of 2 to 3 independent experiments. Abbreviations as in **Figure 1**.

FIGURE 3 Propionate Modulates Tregs in the cLP and Colonic dLNs by Promoting Treg Differentiation



outer diameter of the aneurysm was significantly decreased by SCFAs in comparison with sodium chloride (**Figures 2B and 2D**). Moreover, EVG staining also showed significantly less elastin degradation in SCFA-treated mice than in control mice (**Figures 2C and 2E**). Furthermore, immunohistochemistry staining indicated reduced MMP2 and MMP9 expression and reduced CD3⁺ T cell and CD68⁺ macrophage infiltrations in SCFA-treated mice compared with control mice (**Figures 2F to 2I, Supplemental Figures 4 and 5**).

PROPIONATE PROMOTES TREG DIFFERENTIATION IN THE COLONIC LAMINA PROPRIA. Because SCFAs have been reported to expand Tregs,⁹⁻¹¹ we administered SCFAs to SPF mice without AAA induction for 4 weeks. As reported previously, Tregs are abundant in gut-associated lymphoid tissue,¹⁹ which comprises Peyer's patches (PPs, in the small intestine), the small intestinal lamina propria (SI-LP), the colonic lamina propria (cLP), and mesenteric lymph nodes.²⁰ Mesenteric lymph nodes include several lymph nodes that are compartmentalized to drain lymph from the colon and small intestine.^{20,21} To differentiate the lymph drainage of the colon from small intestine, we injected Evans blue dye into the subserosa of colon and localized the draining lymph nodes (dLNs) of the colon (**Figure 3A**). Intriguingly, we found that Tregs in the small intestine-associated lymphoid system, including Peyer's patches, SI-LP, and small intestinal dLNs, were not changed after the oral administration of SCFAs (**Supplemental Figures 6A to 6C**). Consistent with a previous report,⁹ SCFAs did not increase the proportion of Tregs in the peripheral blood and spleen (**Supplemental Figures 6D and 6E**).

We administered a representative propionate to SPF mice without AAA induction for 4 weeks for further study. We found that Tregs in the cLP (cLP-Tregs) and colonic dLNs were significantly expanded by propionate (**Figures 3B and 3C**). To elucidate the mechanism by which propionate expanded cLP-Tregs,

we examined the expression of the nuclear proliferation antigen Ki67 in cLP-Tregs by flow cytometry and found no significant difference between groups (**Figure 3D**). CD4⁺CD25⁺CD62L^{hi}CD44⁻ naive T cells were cultured under Foxp3⁺ Treg polarization conditions in vitro in the absence or presence of propionate. The result showed that propionate promoted Treg differentiation in the presence of transforming growth factor- β and interleukin-2 (**Figure 3E**). These results indicate that propionate did not promote in situ proliferation of cLP-Tregs, but promote the differentiation of Tregs.

TREG-DEPENDENT ALLEVIATION OF AAA BY PROPIONATE.

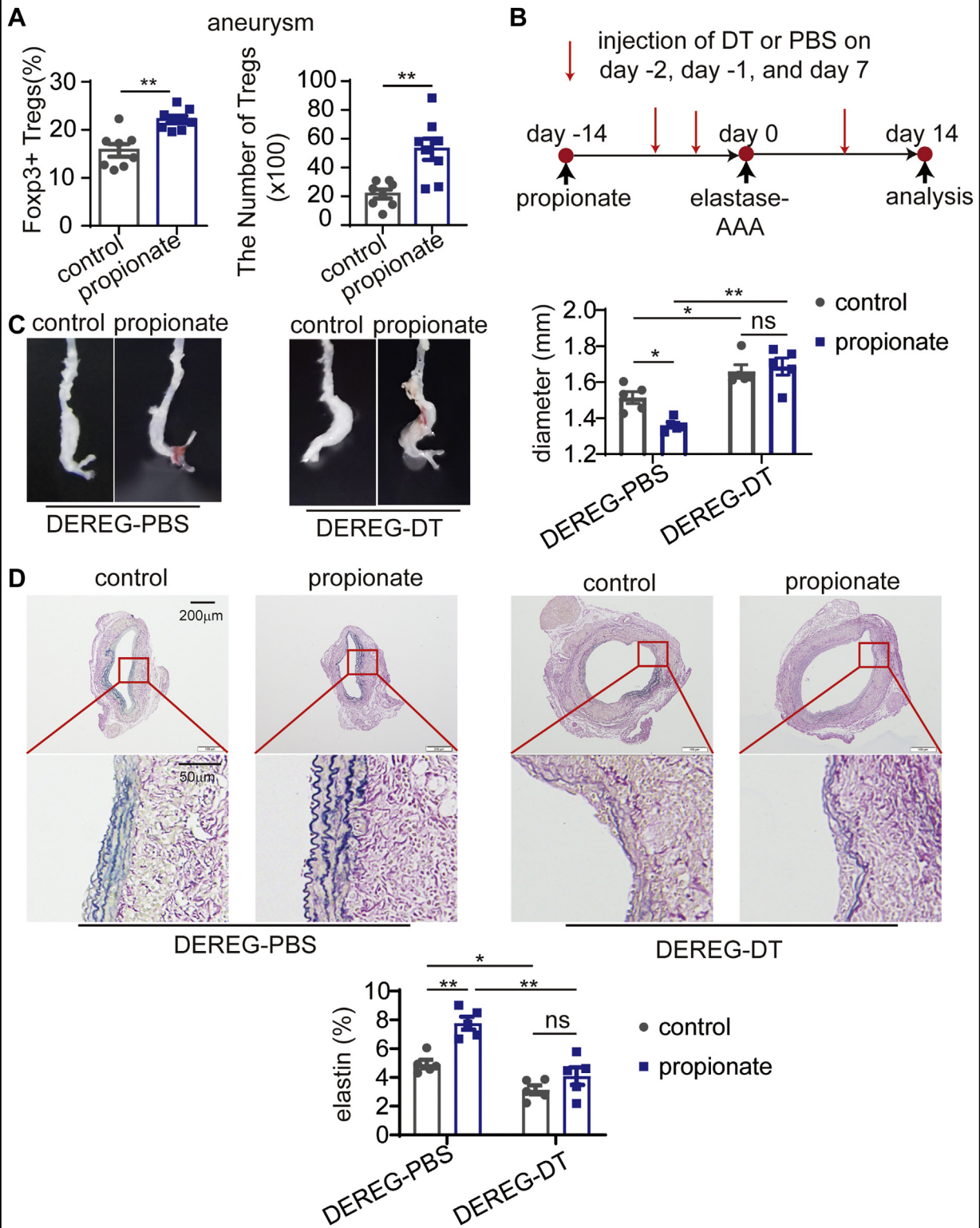
To determine whether the protection against AAA by propionate is related to Tregs, we examined Treg accumulation in the aneurysms of propionate- and control-treated elastase-induced AAA mice. We found that propionate increased both the percentage and number of Foxp3⁺ Tregs in the aneurysms (**Figure 4A**). To confirm this result, acetate, propionate, or butyrate was administered to mice with Ca₃(PO₄)₂-induced AAA, and the percentage of Foxp3⁺ Tregs in the aneurysm was found increased (**Supplemental Figure 7**).

To determine whether the protection against AAA by propionate was Treg-dependent, the mice termed "depletion of regulatory T cell" (DEREG) expressing a diphtheria toxin (DT) receptor under the control of the foxp3 gene locus were used. We then intraperitoneally injected DT to selectively deplete Foxp3⁺ Tregs or PBS as control (**Figure 4B**). DT-treated DEREG mice showed more severe aneurysmal enlargement than PBS-treated mice regardless of propionate or sodium chloride treatment (**Figure 4C**). Moreover, propionate attenuated aneurysmal enlargement in DEREG mice treated with PBS. However, propionate did not attenuate aneurysmal enlargement in DEREG mice treated with DT (**Figure 4C**). Propionate did not reduce elastin degradation in DEREG mice treated with DT, either (**Figure 4D**).

FIGURE 3 Continued

(A) The intestine of an anesthetized C57BL/6J mouse was exposed, and Evans blue dye was injected into the sub-serosal layer. The 3 colonic dLNs (**arrowheads with number**) were localized and distinguished from the small intestinal dLNs. **(B to D)** C57BL/6J mice of SPF grade were administered sodium chloride (control mice), or propionate via their drinking water without AAA induction for 4 weeks before sacrifice. **(B)** Representative contour plots of gating of cLP-Tregs and the percentage of Foxp3⁺ Tregs among CD4⁺ T cells in the cLP (n = 9-10) determined by flow cytometry. **(C)** The percentage of Foxp3⁺ Tregs among CD4⁺ T cells in the colonic dLNs (n = 8) determined by flow cytometry. **(D)** Representative contour plots and the percentage of Ki67⁺ Tregs among Foxp3⁺ Tregs in the cLP determined by flow cytometry (n = 9-10). **(E)** The percentage of Foxp3⁺ Tregs among CD4⁺ T cells induced in vitro from CD4⁺CD25⁺CD62L^{hi}CD44⁻ naive T cells at different conditions as indicated (n = 4). Each **symbol in B to D** represents a value from an individual mouse. *P < 0.05, **P < 0.01. Error bars represent the mean \pm SEM. Unpaired Student's *t*-test (**B to D**) or 2-way ANOVA followed by Bonferroni's multiple comparisons test (**E**). Data shown in **B to D** are representative of 2 independent experiments. cLP = colonic lamina propria; dLNs = draining lymph nodes; ns = not significant.

FIGURE 4 Propionate Increases the Accumulation of Tregs in Aneurysms and Protects Against Elastase-Induced AAA in a Treg-Dependent Manner



Continued on the next page

The anti-CD25 immunoglobulin G (IgG) (PC61), which depletes CD25⁺ cells, including CD25⁺ Tregs, was also used in this experiment. We intraperitoneally injected the anti-CD25 IgG or an isotype control into elastase-induced AAA mice (Supplemental Figure 8A). Tregs in the blood and aneurysm were depleted effectively (Supplemental Figure 8B). In this experiment, propionate did not attenuate aneurysmal enlargement in anti-CD25 IgG-treated mice, but attenuated aneurysmal enlargement in mice treated with the isotype control (Supplemental Figure 8C). Propionate did not reduce elastin degradation in anti-CD25 IgG-treated mice, either (Supplemental Figure 8D). Taken together, this Treg depletion experiment with anti-CD25 IgG showed a congruent result with the DEREg mice experiment, demonstrating the Treg-dependent alleviation of AAA by propionate.

PROPIONATE PROMOTES THE RECIRCULATION OF cLP-TREGS. Because propionate only expands Tregs in cLP and colonic dLNs, but not the small intestine, blood, or spleen, we hypothesized that the increased Tregs in the inflamed aorta are attributable to the recirculation of cLP-Tregs. As reported previously, lymphocytes exit from cLP to dLNs and then enter the blood to fulfill the recirculation process.²⁰ The recirculation of Tregs from cLP was detected using KikGR transgenic mice, which universally express a photoconvertible green fluorescent reporter protein (Kik-green⁺) that turns red (Kik-red⁺) after exposure to 405 nm UV light. The colons of KikGR mice were exposed to UV light for 20 minutes. Tregs in adjacent organs, including colonic dLNs, SI-LP, small intestinal dLNs, and circulating blood, were analyzed immediately after exposure to UV light. As expected, very few Tregs were converted to Kik-red⁺ cells in colonic dLNs, SI-LP, small intestinal dLNs, and circulating blood (Supplemental Figure 9A). To compare the efficacies of photoconversion (phC), mice treated with the control or propionate were sacrificed immediately

after phC. More CD4⁺CD25⁺ Tregs in the cLP were detected in the propionate group than in the control group, but the percentage of Kik-red⁺ Tregs among CD4⁺CD25⁺ Tregs did not differ between the 2 groups (Supplemental Figure 9B).

To compare the recirculation of Tregs from the cLP in propionate-treated and control mice, Kik-red⁺ Tregs in the cLP, colonic dLNs, blood, and aneurysms were examined 36 hours after phC (Figure 5A). We found that fewer Kik-red⁺ Tregs were retained in the cLP of propionate-treated mice than in that of control mice (Figures 5B and 5C). In addition, more Kik-red⁺ Tregs were observed in the colonic dLNs, blood, and aneurysms of propionate-treated mice than in those of control mice (Figures 5B and 5D). These results indicate that propionate promotes Tregs migration from the cLP to the aneurysm through the colonic dLNs and blood.

Lymphocytes in the intestine have been reported to move to and from the gut.²² We examined the cell-intrinsic recirculation ability of cLP-Tregs. The expression of C-C chemokine receptor (CCR) 7 on lymphocytes has been reported to mediate lymphocyte egress from peripheral tissue to dLNs.²³ Nevertheless, our results showed that the CCR7 expression on cLP-Tregs was not altered by propionate (Figure 5E).

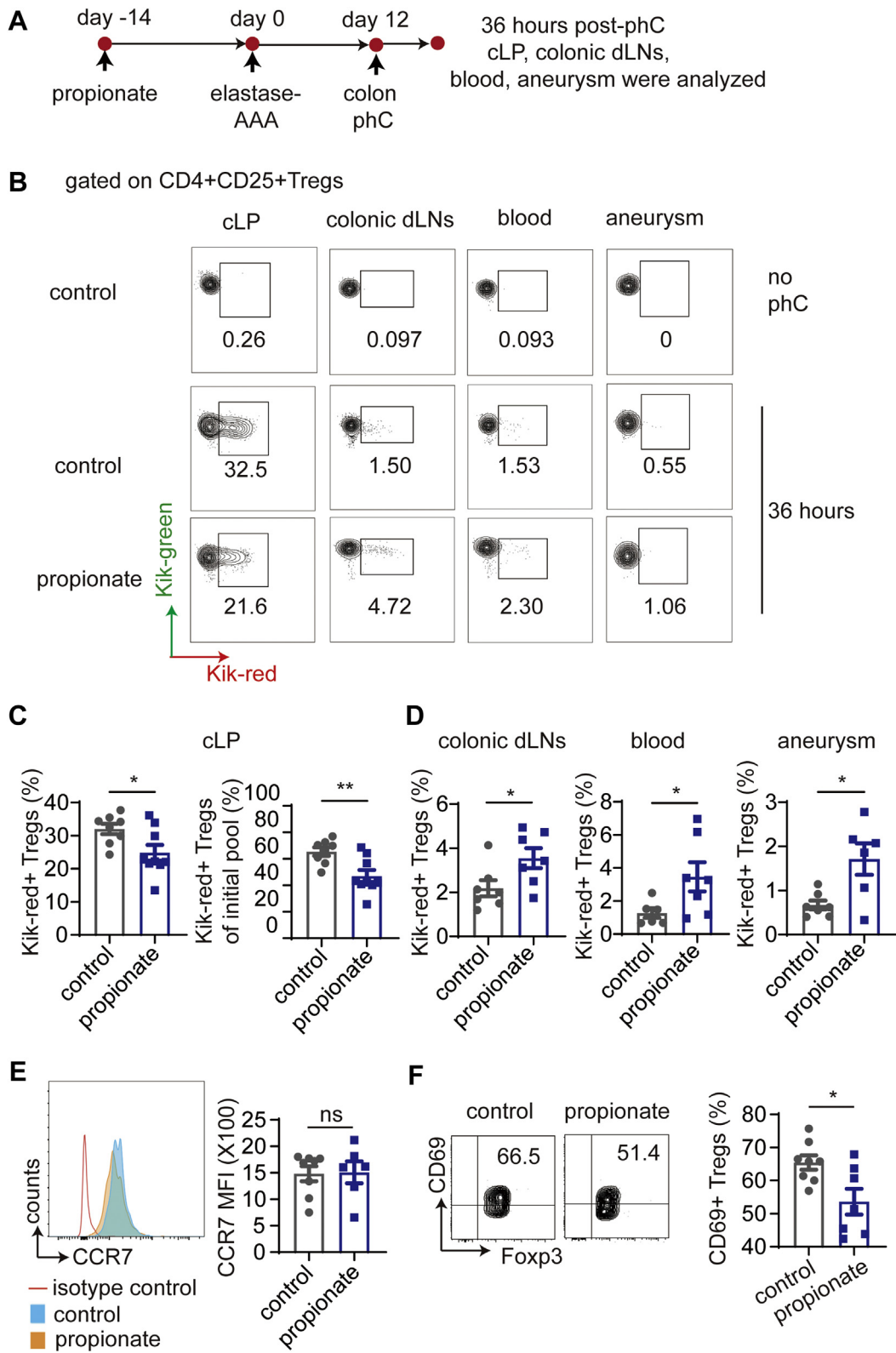
Previous studies have revealed that in a proinflammatory environment, transmembrane C-type lectin CD69, is rapidly induced by local inflammatory mediators. CD69 restricts recirculation by inhibiting sphingosine 1-phosphate receptor-1 (S1P1) on the lymphocyte surface.²⁴ We found that propionate down-regulated CD69 expression on cLP-Tregs (Figure 5F), indicating that it enhanced the recirculation capability of cLP-Tregs.

SURGICAL REMOVAL OF COLONIC dLNs BLOCKS THE RECIRCULATION OF cLP-TREGS. To further confirm that propionate promotes the recirculation of cLP-Tregs to the inflamed aorta via colonic dLNs, we

FIGURE 4 Continued

(A) C57BL/6J mice were administered sodium chloride (control mice), or propionate via their drinking water for 14 days before the induction of AAA by elastase. The mice were sacrificed 14 days after AAA induction for the analysis of Tregs in the aneurysms. The percentage of Foxp3⁺ Tregs among CD4⁺ T cells and the absolute number of Tregs in the aneurysms of mice were determined by flow cytometry (n = 8). (B) Study overview: DEREg mice were administered sodium chloride or propionate from day -14 to day 14, and AAA was induced by elastase on day 0. The injection of DT or PBS was performed on day -2, day -1, and day 7, and the mice were sacrificed on day 14. (C) Representative images of the aneurysms of mice in B and the maximum external diameters of the aneurysms measured ex vivo (n = 5). (D) Representative EVG staining of the aneurysms and the percentage of elastin area (of the total aortic area) (n = 5) calculated from the EVG staining sections. Each symbol represents a value from an individual mouse. In D, a mean value of 4 consecutive sections was calculated. Scale bars are depicted in the images. *P < 0.05, **P < 0.01. Error bars represent the mean ± SEM. Unpaired Student's t-test (A) or 2-way ANOVA followed by Bonferroni's multiple comparisons test (C and D). DEREg = depletion of regulatory T cell; DT = diphtheria toxin; other abbreviations as in Figures 1 and 3.

FIGURE 5 Propionate Facilitates the Recirculation of cLP-Tregs Through Colonic dLNs and Blood to the Aneurysm



performed colonic dLN lymphadenectomy to block the recirculating circuit in C57BL/6J mice (Figure 6A). Two weeks after AAA induction and colonic dLN lymphadenectomy, the percentage of Tregs in the cLP of the propionate-treated mice was higher than that of control mice (Figure 6B). However, the percentage of Tregs infiltrating the aneurysms and the percentage of Tregs in blood did not change in propionate-treated mice (Figure 6C). Evaluations of aneurysmal enlargement and the relative expression of MMPs and proinflammatory mediators in the aneurysms revealed no differences between propionate and control mice (Figures 6D and 6E). In conclusion, these data demonstrate that the recirculation circuit of cLP-Tregs is blocked and that the protective effect of propionate against AAA is abolished after the removal of colonic dLNs.

DISCUSSION

In the present study, we demonstrate that SCFAs protect against $\text{Ca}_3(\text{PO}_4)_2$ -induced and elastase-induced AAA in mice. Treg depletion experiments verified Treg-dependent protection against AAA by propionate. Tracing of cLP-Tregs in KikGR mice provided evidence of cLP-Treg recirculation to the inflamed aorta. The surgical removal of colonic dLNs blocked the recirculation of cLP-Tregs and abolished the protective effects of propionate against AAA. Apart from expanding the pool of cLP-Tregs, propionate alters their cell-intrinsic recirculation ability by down-regulating CD69. Taken together, our results provide a novel perspective on the mechanism by which propionate protects against AAA.

The intriguing finding of our study was the trafficking of cLP-Tregs to dLNs, the bloodstream and the aneurysm. Previous reports on the immunoregulatory role of SCFAs have revealed their protective effects against local colonic inflammation via cLP-Tregs.⁹⁻¹¹ We herein demonstrated that cLP-Tregs were

capable of entering dLNs and accumulating in the inflamed aorta by tracing UV-converted Kik-red⁺ Tregs of KikGR mice. Removal of colonic dLNs supported the conclusion that colonic Tregs recirculate via dLNs and blood circulation.

Researchers have revealed that cLP-Tregs are tissue-resident Tregs with phenotypes, functions, and local sustaining factors that differ from those of circulating Tregs.¹⁹ Nonetheless, in addition to their role in maintaining colon homeostasis, cLP-Tregs can also recirculate to defend against excessive distant inflammation.²² Emerging studies have suggested that lymphocytes dynamically migrate from the gut to distal inflamed organs such as the brain.²⁵⁻²⁷ Our work adds additional evidence, demonstrating that propionate expands the pool of cLP-Tregs and facilitates the exit of cLP-Tregs from the cLP and the entry of cLP-Tregs into dLNs and inflamed aneurysms.

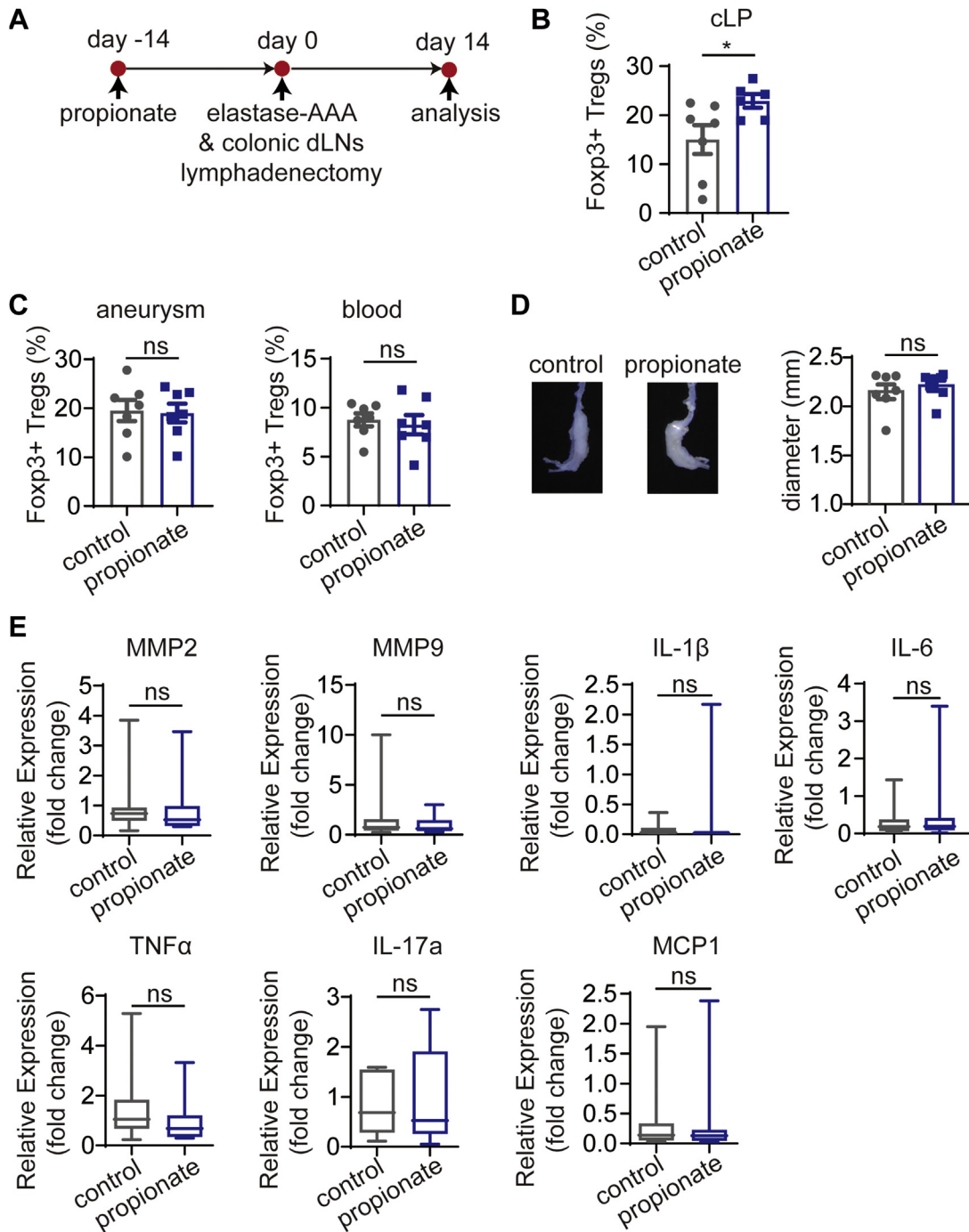
It is now technically feasible to follow a specific cell type from 1 organ or tissue to another in genetically modified mice, such as the KikGR mice used in our study. However, clinically following the migration of Tregs is not currently possible, and we herein propose possible directions for development of novel methods. First, based on the fact that rotavirus specifically infects mature enterocytes in the small intestine and produces local antigen-specific B cells, Rojas et al²⁶ designed an elaborate ELISPOT experiment to detect rotavirus-specific B cells in blood and other distal tissue, and thereby follow B cells from the intestine to other organs. This experiment is inspiring and suggests that intestinal commensal-specific Tregs are present in the blood, which would help us to clinically follow Tregs from intestine to other organs. Second, the identification of organ- or tissue-specific Treg markers will also facilitate the clinical tracing of intestinal Tregs.

Intestinal microbial metabolites serve as tools for communication between the commensal microbes and the immune system. SCFAs are abundantly produced by microbes through fiber fermentation, and this mechanism is related to the epidemiological

FIGURE 5 Continued

(A) Study overview: AAA was induced with elastase in sodium chloride-treated or propionate-treated KikGR mice, and 12 days later, the colons of the mice were exposed to UV light. Kik-red⁺ Tregs from the indicated tissues were examined by flow cytometry 36 hours after pHc. **(B)** Representative contour plots of Kik-red⁺ Tregs in the cLP, colonic dLNs, blood, and aneurysms of mice treated as described in **A**. **(C)** The percentage of Kik-red⁺ Tregs among CD4⁺CD25⁺ Tregs in the cLP and the percentage of Kik-red⁺ Tregs in the cLP normalized to the initial pHc Treg pool (n = 8-9). **(D)** The percentages of Kik-red⁺ Tregs among CD4⁺CD25⁺ Tregs in colonic dLNs (n = 7), blood (n = 6-7), and aneurysms (n = 6-7) 36 hours after the pHc of mice treated as described in **A**. **(E and F)** C57BL/6J mice were administered sodium chloride (control mice), or propionate via their drinking water for 14 days before the induction of AAA by elastase. The mice were sacrificed 14 days after AAA induction for the analysis of cLP-Tregs by flow cytometry. **(E)** Mean fluorescence intensity of CCR7 on cLP-Tregs (n = 6-8). **(F)** The percentage of CD69⁺ Tregs among Foxp3⁺ Tregs in the cLP (n = 7-8). Each **symbol** represents a value acquired from an individual mouse. *P < 0.05, **P < 0.01. Error bars represent the mean ± SEM. Unpaired Student's t-test (**C to F**). Data shown are representative of 2 to 4 independent experiments. MFI = mean fluorescence intensity; pHc = photoconversion; other abbreviations as in Figures 1 and 3.

FIGURE 6 Colonic dLNs Lymphadenectomy Abolishes the Protective Effect of Propionate on Elastase-Induced AAA



(A) Study overview: C57BL/6J mice of SPF grade were administered sodium chloride or propionate for 14 days before the induction of AAA by elastase along with colonic dLNs lymphadenectomy. The mice were sacrificed 14 days after AAA induction. **(B)** The percentage of Fcpx3⁺ Tregs among CD4⁺ T cells in the cLP of mice (n = 6-7). **(C)** The percentage of Fcpx3⁺ Tregs among CD4⁺ T cells in the aneurysms and blood of mice (n = 7). **(D)** Representative images of the aneurysms and the maximum external diameters of the aneurysms (n = 7). **(E)** Relative expression of inflammatory mediators in the aneurysms (n = 8). Each symbol represents a value from an individual mouse. *P < 0.05. Error bars represent the mean ± SEM for **B** to **D**. Data are shown with box-whisker plots for **E**. Unpaired Student's t-test (**B** to **D**). Mann-Whitney U test (**E**). Data shown are representative of 2 independent experiments. Abbreviations as in **Figures 1 and 3**.

correlation of fiber intake with cardiovascular disease.^{28,29} Specific targets for the prevention or treatment of AAA have not yet been identified. The adoptive transfer of Tregs has been shown to ameliorate vascular damage.¹⁸ Prebiotic-based treatment may be an alternative to promote the accumulation of Tregs in the inflamed aorta. Notably, under physiological conditions, SCFAs are abundantly produced from high-fiber foods in the gut, which implies their safety to humans. Direct supplementation of SCFAs may be an effective and economical approach to prevent AAA, as indicated in this study. Additionally, the modification of starch created by chemically linking acetate, propionate, or butyrate to high-amylose maize starch to increase the content of SCFAs has been demonstrated to protect against type 1 diabetes in mice.³⁰ We propose that SCFA-enriched starch can be used as a medicinal food for patients at high risk of developing AAA.

STUDY LIMITATIONS. The limitations of our study merit consideration. Epidemiological data show that the incidence of AAA is approximately 4 to 5 times higher among men than women. The incidence of AAA in female mice is much lower than that in male mice in all tested experimental AAA models.³¹ Therefore, we designed and performed the experiments using only male mice, meaning that the results may not be fully generalizable to female mice. Emerging studies show the distinct actions of immune cells in male and female mice in cardiovascular settings.³²⁻³³ Further studies including female mice and comparing male and female mice are warranted.

We performed Treg depletion experiments with both DERE mice and anti-CD25 IgG, which were widely used in previous research. DERE mice are genetically modified to selectively and effectively deplete foxp3⁺ Tregs with DT injection, and anti-CD25 IgG also depletes Foxp3⁺ Tregs effectively in our experiment. Though anti-CD25 IgG is also widely used in Treg depletion experiment as reported, there is a possibility that anti-CD25 IgG depletes, not only CD25⁺Foxp3⁺ Tregs, but also activated effector CD8⁺ and CD4⁺ T cells, which were reported to be involved in the pathogenesis of AAA. Two Treg depletion

experiments showed congruent results and convincingly proved Treg-dependent protection against AAA by propionate.

CONCLUSIONS

We herein revealed how SCFA-expanded colonic Tregs, one of the largest Treg reservoirs in the body, alleviate AAA. This finding has translational meaning for the prevention and treatment of AAA with active intestinal microbial metabolites.

ACKNOWLEDGMENTS The authors thank the faculty of the animal facility of Huazhong University of Science and Technology (Wuhan, China) for care of the mice.

FUNDING SUPPORT AND AUTHOR DISCLOSURES

This work was supported by the National Natural Science Foundation of China grants No. 81720108005, and 82030016 (Dr Cheng), No. 81770503 and 81400364 (Dr Xia), and No. 81670361 and 81974037 (Dr Tang), and the 2017 Chang Jiang Scholars Program T2017073 (Dr Cheng). The authors have reported that they have no relationships relevant to the contents of this paper to disclose.

ADDRESS FOR CORRESPONDENCE: Dr Xiang Cheng, Department of Cardiology, Union Hospital, Tongji Medical College, Huazhong University of Science and Technology, and Key Laboratory of Biological Targeted Therapy of the Ministry of Education, 1277 Jiefang Road, Jianghan District, Wuhan 430022, Hubei, China. E-mail: nathancx@hust.edu.cn.

PERSPECTIVES

COMPETENCY IN MEDICAL KNOWLEDGE: The intestinal microbial metabolite propionate protects mice against Ca₃(PO₄)₂-induced and elastase-induced AAA by promoting Tregs in cLP to recirculate to the aneurysm.

TRANSLATIONAL OUTLOOK: Our study in mice with AAA suggests that intestinal microbial metabolites SCFAs might be a promising strategy for the prevention of AAA progression.

REFERENCES

- Kent KC. Abdominal aortic aneurysms. *N Engl J Med*. 2014;371:2101-2108.
- Nordon IM, Hinchliffe RJ, Loftus IM, Thompson MM. Pathophysiology and epidemiology of abdominal aortic aneurysms. *Nat Rev Cardiol*. 2011;8:92-102.
- Dale MA, Ruhlman MK, Baxter BT. Inflammatory cell phenotypes in AAAs: their role and potential as targets for therapy. *Arterioscler Thromb Vasc Biol*. 2015;35:1746-1755.
- Meng X, Yang JM, Zhang K, et al. Regulatory T cells prevent angiotensin II-induced abdominal aortic aneurysm in apolipoprotein E knockout mice. *Hypertension*. 2014;64:875-882.
- Zhou Y, Wu WX, Lindholt JS, et al. Regulatory T cells in human and angiotensin II-induced mouse abdominal aortic aneurysms. *Cardiovasc Res*. 2015;107:98-107.

6. Erbel R, Aboyans V, Boileau C, et al. 2014 ESC guidelines on the diagnosis and treatment of aortic diseases: document covering acute and chronic aortic diseases of the thoracic and abdominal aorta of the adult. The Task Force for the Diagnosis and Treatment of Aortic Diseases of the European Society of Cardiology (ESC). *Eur Heart J*. 2014;35:2873-2926.
7. Tang WHW, Bäckhed F, Landmesser U, Hazen SL. Intestinal microbiota in cardiovascular health and disease. *J Am Coll Cardiol*. 2019;73:2089-2105.
8. Koh A, De Vadder F, Kovatcheva-Datchary P, Bäckhed F. From dietary fiber to host physiology: short-chain fatty acids as key bacterial metabolites. *Cell*. 2016;165:1332-1345.
9. Smith PM, Howitt MR, Panikov N, et al. The microbial metabolites, short-chain fatty acids, regulate colonic Treg cell homeostasis. *Science*. 2013;341:569-573.
10. Furusawa Y, Obata Y, Fukuda S, et al. Commensal microbe-derived butyrate induces the differentiation of colonic regulatory T cells. *Nature*. 2013;504:446-450.
11. Arpaia N, Campbell C, Fan XY, et al. Metabolites produced by commensal bacteria promote peripheral regulatory T-cell generation. *Nature*. 2013;504:451-455.
12. Marques FZ, Nelson E, Chu PY, et al. High-fiber diet and acetate supplementation change the gut microbiota and prevent the development of hypertension and heart failure in hypertensive mice. *Circulation*. 2017;135:964-977.
13. Bartolomaeus H, Balogh A, Yakoub M, et al. Short-chain fatty acid propionate protects from hypertensive cardiovascular damage. *Circulation*. 2019;139:1407-1421.
14. Kasahara K, Krautkramer KA, Org E, et al. Interactions between Roseburia intestinalis and diet modulate atherogenesis in a murine model. *Nat Microbiol*. 2018;3:1461-1471.
15. Brandsma E, Kloosterhuis NJ, Koster M, et al. A pro-inflammatory gut microbiota increases systemic inflammation and accelerates atherosclerosis. *Cir Res*. 2018;124:94-100.
16. Tang TWH, Chen HC, Chen CY, et al. Loss of gut microbiota alters immune system composition and cripples post-infarction cardiac repair. *Circulation*. 2019;139:647-659.
17. Bhamidipati CM, Mehta GS, Lu G, et al. Development of a novel murine model of aortic aneurysms using peri-adventitial elastase. *Surgery*. 2012;152:238-246.
18. Li J, Xia N, Wen S, et al. IL (interleukin)-33 suppresses abdominal aortic aneurysm by enhancing regulatory T-Cell expansion and activity. *Arterioscler Thromb Vasc Biol*. 2019;39:446-458.
19. Panduro M, Benoist C, Mathis D. Tissue Tregs. *Annu Rev Immunol*. 2016;34:609-633.
20. Mowat AM, Agace WW. Regional specialization within the intestinal immune system. *Nat Rev Immunol*. 2014;14:667-685.
21. Esterhazy D, Canesso MCC, Mesin L, et al. Compartmentalized gut lymph node drainage dictates adaptive immune responses. *Nature*. 2019;569:126-130.
22. Morton AM, Sefik E, Upadhyay R, Weissleder R, Benoist C, Mathis D. Endoscopic photoconversion reveals unexpectedly broad leukocyte trafficking to and from the gut. *Proc Natl Acad Sci U S A*. 2014;111:6696-6701.
23. Förster R, Davalos-Misslitz AC, Rot A. CCR7 and its ligands: balancing immunity and tolerance. *Nat Rev Immunol*. 2008;8:362-371.
24. Shioh LR, Rosen DB, Brdicková N, et al. CD69 acts downstream of interferon- α/β to inhibit SIP1 and lymphocyte egress from lymphoid organs. *Nature*. 2006;440:540-544.
25. Benakis C, Brea D, Caballero S, et al. Commensal microbiota affects ischemic stroke outcome by regulating intestinal $\gamma\delta$ T cells. *Nat Med*. 2016;22:516-523.
26. Rojas OL, Pröbstel AK, Porfilio EA, et al. Recirculating intestinal IgA-producing cells regulate neuroinflammation via IL-10. *Cell*. 2019;176:610-624.
27. Fitzpatrick Z, Frazer G, Ferro A, et al. Gut-educated IgA plasma cells defend the meningeal venous sinuses. *Nature*. 2020;587:472-476.
28. Stackelberg O, Björck M, Larsson SC, Orsini N, Wolk A. Fruit and vegetable consumption with risk of abdominal aortic aneurysm. *Circulation*. 2013;128:795-802.
29. Du H, Li L, Bennett D, et al. Fresh fruit consumption and major cardiovascular disease in China. *N Engl J Med*. 2016;374:1332-1343.
30. Mariño E, Richards JL, McLeod KH, et al. Gut microbial metabolites limit the frequency of autoimmune T cells and protect against type 1 diabetes. *Nat Immunol*. 2017;18:552-562.
31. Robinet P, Milewicz DM, Cassis LA, Leeper NJ, Lu HS, Smith JD. Consideration of sex differences in design and reporting of experimental arterial pathology studies: a statement from the ATVB Council. *Arterioscler Thromb Vasc Biol*. 2018;38:292-303.
32. Man JJ, Beckman JA, Jaffe IZ. Sex as a biological variable in atherosclerosis. *Circ Res*. 2020;126:1297-1319.
33. Haider A, Bengs S, Luu J, et al. Sex and gender in cardiovascular medicine: presentation and outcomes of acute coronary syndrome. *Eur Heart J*. 2020;41:1328-1336.

KEY WORDS abdominal aortic aneurysm, colonic regulatory T cell, propionate, recirculation, short-chain fatty acids

APPENDIX For an expanded Methods section and supplemental figures, please see the online version of this paper.